Published in final edited form as:
Soft Matter. 2012 January 14; 8(2): 481–487. doi:10.1039/C1SM06105D.

Thermoresponsive nanocomposite double network hydrogels†

Ruochong Fei, **Jason Thomas George**, **Jeehyun Park**, and **Melissa Ann Grunlan***
Department of Biomedical Engineering, Materials Science & Engineering Program, Texas A&M University, 3120 TAMU, College Station, TX, USA

Abstract

The utility and efficacy of thermoresponsive poly(*N*-isopropylacrylamide) (PNIPAAm) hydrogels as smart materials is limited by their physical properties. In this study, we sought to design PNIPAAm nanocomposite hydrogels which displayed enhanced mechanical properties as well as deswelling–reswelling kinetics but without reducing equilibrium swelling or altering the convenient volume phase transition temperature (*VPTT*) of PNIPAAm. PNIPAAm hydrogels were formed as double networks (DN) comprised of a tightly crosslinked 1st network and a loosely crosslinked 2nd network. In addition, polysiloxane nanoparticles of two different average diameters (~50 nm and ~200 nm) were incorporated during formation of the 1st or 2nd network. The influence of the hydrogel composition on *VPTT*, morphology, equilibrium swelling, deswelling–reswelling kinetics and mechanical properties was evaluated. We observed that DN hydrogels formed with ~200 nm polysiloxane nanoparticles introduced during formation of the 1st network achieved the best combination of the desired properties.

Introduction

Thermal modulation reversibly switches crosslinked poly(*N*-isopropylacrylamide) (PNIPAAm) hydrogels between a water-swollen, hydrophilic state and a deswollen, hydrophobic state.[1,2] A volume phase transition temperature (*VPTT*) of ~33–35 °C makes PNIPAAm hydrogels particularly useful to prepare "smart" materials for biological applications.[3–6] These applications include microfluidic actuation,[7–10] separation,[7,11,12] controlled drug delivery[7,13–15] and controlled detachment of adsorbed cells and proteins for cell sheet tissue engineering,[7,16,17] anti-fouling coatings,[18–20] and "self-cleaning" membranes for implanted biosensors.[21–24]

In these applications, conventional PNIPAAm hydrogels prepared *via* copolymerization of *N*-isopropylacrylamide (NIPAAm) and a crosslinker such as *N,N′*-methylenebisacrylamide (BIS) have limited efficacy due to poor mechanical properties as well as slow deswelling–reswelling kinetics (*i.e.* thermosensitivity).[25] It is typical to employ strategies which reduce equilibrium swelling in order to improve hydrogel mechanical properties such as increasing crosslink density[26,27] and introducing discrete fillers.[28] However, a highly swollen state is critical for certain applications involving transport or separation. In addition, many strategies useful to enhance the thermosensitivity of PNIPAAm hydrogels (without altering the *VPTT*) diminish mechanical properties, including: comb-type networks,[29–31] heterogeneous morphologies,[32–35] poration[36–39] or open channel structures.[40]

†Electronic supplementary information (ESI) available: Table S1. See DOI: 10.1039/c1sm06105d/

mgrunlan@tamu.edu; Fax: +1 979 845 4450; Tel: +1 979 845 2406.

Nanocomposite hydrogels, including those based on PNIPAAm, have attracted recent attention, particularly for biological applications.[41,42] PNIPAAm-based nanocomposite hydrogels have been prepared with various fillers such as iron oxide nanoparticles,[43] gold nanoparticles,[44] silicate nanoplatelets,[45,46] graphene,[47,48] carbon nanotubes[49] and silica.[50] We recently reported PNIPAAm nanocomposite hydrogels prepared by introduction of hydrophobic polysiloxane nanoparticles with average diameters of ~50 nm[51] and ~200 nm.[52] Without changing the *VPTT*, the polysiloxane nanoparticles produced an increase in hydrogel rigidity. However, this was at least due in part to a decrease in equilibrium swelling of the nanocomposite hydrogels. Notably, we also observed that nanocomposite hydrogels containing ~50 nm particles exhibited an exceptionally enhanced rate of deswelling.[51]

In this study, we sought to design a PNIPAAm nanocomposite hydrogel which displayed enhanced mechanical properties as well as deswelling–reswelling kinetics and without reducing equilibrium swelling or altering the *VPTT*. Compared to conventional or single network (SN) hydrogels, double network (DN) network hydrogels are associated with enhanced mechanical properties as well as a high degree of swelling.[53,54] DN hydrogels are a class of interpenetrating polymer networks (IPNs) comprised of two highly asymmetrically crosslinked networks. Gong and co-workers reported the first DN hydrogels consisting of a tightly crosslinked, ionizable 1st network comprised of poly(2-acrylamide-2-methyl-propane sulfonic acid) (PAMPS) and a sparsely crosslinked, neutral 2nd network comprised of poly(acrylamide) (PAAm).[55,56] DN hydrogels consisting of poly(ethylene oxide) (PEO) and poly (acrylic acid) (PAA) have also been prepared which are essentially the inverse of those prepared by Gong *et al.*[57] These are comprised of a tightly crosslinked, neutral 1st network of PEO and a loosely crosslinked, ionizable 2nd network of PAA. Several other DN hydrogels have been reported but are similarly non-thermoresponsive.[58,59] Zhang *et al.* reported PNIPAAm IPNs but the crosslinking designs do not qualify them as DNs.[60] Also, while these PNIPAAm IPNs achieved enhanced mechanical properties, equilibrium swelling was correspondingly decreased.

Herein, we report thermoresponsive PNIPAAm DN hydrogels containing inorganic polysiloxane nanoparticles (Table 1, Fig. 1). Colloidal polysiloxane nanoparticles with average diameters of ~50 nm[51] and ~200 nm[52] prepared *via* emulsion polymerization were utilized. Nanocomposite DN hydrogels were prepared with a tightly crosslinked PNIPAAm 1st network and a loosely crosslinked PNIPAAm 2nd network by altering the amount of BIS crosslinker. Nanoparticles were introduced during the formation of the 1st or 2nd network. The *VPTT*, morphology, equilibrium swelling, deswelling–reswelling kinetics, and mechanical properties were evaluated.

Experimental

Materials

Octamethylcyclotetrasiloxane (D_4) and 1,3,5,7-tetra-methyl-1,3,5,7-tetravinylcyclotetrasiloxane (D_4^{vi}) were purchased from Gelest, Inc. Brij 35, Brij 78, *N*-isopropylacrylamide (NIPAAm, 97%) and Tergitol NP-40 (70% in H_2O) were obtained from Aldrich. Dodecylbenzenesulfonic acid (DBSA, BIO-SOFT® S-101) was purchased from Stepan Co. Potassium persulfate ($K_2S_2O_8$) was purchased from Mallinchrodt Chemicals. *N,N′*-methylenebisacrylamide (BIS, 99%) was purchased from ACROS. 1-[4-(2-Hydroxy)-phenyl]-2-hydroxy-2-methyl-1-pro-pane-1-one (Irgacure 2959) was purchased from Ciba.

Synthesis of crosslinked polysiloxane colloidal nanoparticles

Crosslinked polysiloxane nanoparticles having two different average diameters (54 nm[51] and 219 nm[52]) were prepared as previously reported.

Preparation of single network (SN) hydrogels

SN hydrogels were prepared via in situ photocure of aqueous precursor solutions containing NIPAAm monomer, BIS crosslinker, Irgacure-2959 photoinitiator, DI water and, optionally, crosslinked polysiloxane nanoparticles (2 wt% solid nanoparticles based on NIPAAm wt). In a 50-mL round bottom (rb) flask equipped with a Teflon-covered stir bar, NIPAAm (1.0 g), BIS (0.04 g), and Irgacure-2959 (0.08 g) were dissolved in DI water (the total volume equal to 7 mL including the volume of water introduced by the nanoparticle emulsion). Finally, the required amount of nanoparticle emulsion was optionally added.

Hydrogel sheets were prepared by pipetting the precursor solution into a rectangular mold formed by sandwiching polycarbonate spacers (1.5 mm thick) between two clamped glass microscope slides. The mold was submerged in an ice water bath (~7 °C) and subjected to UV light (UV-Transilluminator, 6 mw/cm^2, 365 nm) for 30 min. After removal from the mold, the hydrogel sheet was rinsed with DI water and then soaked in DI water for 2 days with daily water changes to remove impurities.

For tensile tests, hydrogels were prepared with a “ring” geometry. First, hydrogels were prepared as a hollow tube with a double walled tubular mold composed of an inner glass mandrel (diameter = 3.2 mm) and an outer glass cylinder (diameter = 7.9 mm) secured with machined Teflon stoppers at each end. After removing one stopper, the tubular mold was filled with the precursor solution, stoppered, and photocured while submerged in an ice water bath (~7 °C) for 30 min under constant rotation such that each surface point received equal UV intensity and exposure time. The hydrogel tube was removed from the mold and similarly purified as above. For tensile tests of *SN*, ~ 3 mm wide pieces were cut from the central portion of the resulting hydrogel tube.

Preparation of double network (DN) hydrogels

The designated SN hydrogel was soaked in a solution of NIPAAm (6.0 g), BIS (0.012 g), Irgacure-2959 (0.24 g), DI water (the total volume equal to 21 mL including the volume of water introduced by the nanoparticle emulsion) and optionally cross-linked polysiloxane nanoparticles (2 wt% solid nanoparticles based on NIPAAm wt) for 24 h. The hydrogel sheet was then transferred to a rectangular mold (2.3 mm thick), photocured and purified as above.

For tensile tests, DN hydrogels with a ring geometry were prepared by soaking the previously prepared SN hydrogel tube in the aforementioned solution as above. The hydrogel tube was then transferred to a double walled tubular mold composed of an inner glass mandrel (diameter = 3.2 mm) and an outer glass cylinder (diameter = 12.5 mm), secured with Teflon stoppers at each end and cured as above (~7 °C, 30 min). Following purification, the central portion of the hydrogel tube was cut into ~ 3 mm wide pieces to produce the ring specimens.

Extent of crosslinking

The amount of uncrosslinked material in select hydrogels was determined by weight loss following soaking in dichloromethane (CH_2Cl_2). For a given hydrogel, three hydrogel discs (13 mm diameter, 1.5 mm thickness) were punched from a single hydrogel sheet with a die and dried in a vacuum oven [30 in. Hg, room temperature (RT), 24 h] and weighed. Each dried discs was soaked in 10 mL of CH_2Cl_2 for 24 h and weighed after similarly drying in a

vacuum oven. The percentage of uncrosslinked material was calculated as the average weight difference of the extracted *versus* unextracted weight divided by the unextracted weight.

Volume phase transition temperature (VPTT)

The *VPTT* of swollen hydrogels was determined by differential scanning calorimetry (DSC, TA Instruments Q100). Water-swollen hydrogels were blotted with Kim Wipe and a small piece sealed in a hermetic pan. After cooling to −50 °C, the temperature was increased to 50 °C at a rate of 3 °C min^{-1} for 2 cycles. The resulting endothermic phase transition peak is characterized by the initial temperature at which the endotherm starts (T_o) and the peak temperature of the endotherm (T_{max}). Reported data is from the 2nd cycle.

Morphology

To retain their morphology, swollen hydrogel specimens were immersed in liquid nitrogen and subsequently freeze-dried with a lyophilizer (Labconco Centri Vap Gel Dryer System) overnight. Specimen cross-sections were subjected to Pt-sputter coating and viewed with a field emission scanning electron microscope (FEI Quanta 600 FE-SEM) at an accelerated electron energy of 10 keV.

Equilibrium swelling

Three discs (13 mm diameter) were punched from a single sheet with a die. Each disc was placed in a sealed vial containing 20 mL DI water, immersed in a temperature controlled water bath for 24 h at the designated temperature (10–50 °C), removed, blotted with a Kim Wipe to remove surface water and weighed (W_t). After the last measurement, each disc was vacuum dried (30 in. Hg, 60 °C, 24 h) and weighed (W_d). Equilibrium swelling ratio (SR) is defined as: $SR = W_t/W_d$.

Kinetic deswelling

Three discs (13 mm diameter) were prepared as above. Each disc was placed in a sealed vial containing 20 mL DI water, immersed in a water bath for 24 h at 22 °C to reach equilibrium (W_s) and quickly transferred into a 50 °C water bath. At 10, 20, 40, 80, 120, 180 min, each disc was removed, blotted with a Kim Wipe, immediately weighed (W_t) and returned to the vial for subsequent measurements. After 180 min, the discs were dried in a vacuum oven (30 in. Hg, 60 °C, 24 h) and weighed (W_d). Water retention (WR) is defined as: $WR = (W_t - W_d)/W_s$.

Kinetic re-swelling

Three discs (13 mm diameter) were prepared as above. Each disc was placed in an open vial, dried in a vacuum oven (30 in. Hg, 60 °C, 24 h) and weighed (W_d). To each vial was added 20 mL DI water and the sealed vial immersed in a water bath at 22 °C. At 10, 20, 40, 80, 120, 200, 320, 450 and 640 min, each disc was removed, blotted with a Kim Wipe and weighed (W_t). Kinetic reswelling ratio is defined as: $SR = W_t/W_d$.

Dynamic mechanical analysis (DMA)

Five discs (13 mm diameter) were prepared as above. DMA of discs was measured in the compression mode with a dynamic mechanical analyzer (TA Instruments Q800) equipped with parallel-plate compression clamp with a diameter of 40 mm (bottom) and 15 mm (top). The swollen disc (13 mm diameter) was blotted with a Kim Wipe, clamped between the parallel plates and silicone oil placed around the exposed hydrogel edge to prevent dehydration. Following equilibration below the VPTT at 25 °C (5 min), the specimens were tested in a multi-frequency-strain mode (1 to 25 Hz).

Compression tests

Three discs (13 mm diameter) were prepared as above. Compressive tests were performed with an Instron 3340 at RT. A swollen disc (13 mm diameter) was blotted with a Kim Wipe and clamped between the parallel plates with an initial pre-load force of ~0.5 N. Compressive strain was applied at a rate of 1 mm min^{-1} until the disc fractured. The following parameters were determined: (1) compressive modulus; (2) ultimate compressive strength (*UCS*), and (3) % strain at break. The modulus was obtained from the slope of the stress-strain curve between 0 and 10% strain.[58]

Tensile tests

A ring geometry rather than a rectangular strip or dog bone was used to measure tensile properties for improved accuracy.[52,61] Three hydrogel rings (~3 mm width) were cut from the central portion of the designated hydrogel tube using a razor blade and dimensions measured with an electronic caliper. The ring was blotted with a Kim Wipe and loaded onto custom aluminum bars gripped directly into DMA tension clamps so that the upper and lower bars were located inside the ring. At RT, samples were subjected to a constant strain (1 mm min^{-1}) until they broke at the center of one side of the ring. Stress was calculated from the measured force divided by the cross-sectional area of two rectangles with sides equal to the width and wall thickness of the ring. The gauge length corresponded to the outer diameter of the ring less the wall thickness. The following parameters were determined: (1) tensile modulus, (2) ultimate tensile strength (*UTS*), and (3) % strain at break. The tensile modulus was obtained from the slope of the linear part of the stress-strain curve between 0 and 10% strain. The *UTS* represents the maximum stress prior to failure. % Strain at break was calculated from the measured displacement divided by the gauge length.

Result and discussion

Preparation of SN and DN hydrogels

SN hydrogels (including "*SN*") were formed by photo-polymerization of aqueous solutions containing NIPAAm monomer and BIS crosslinker (4 wt% based on NIPAAm) and optionally polysiloxane nanoparticles (Table 1, Fig. 1). DN hydrogels (including "*DN*") were formed sequentially in two steps by swelling the designated SN hydrogel with an aqueous solution containing NIPAAm and BIS crosslinker (0.2 wt% based on NIPAAm) and optionally polysiloxane nanoparticles followed by subsequent photocure. For all DN hydrogels, the % uncrosslinked material extracted was less than 2% (Table S1). The DN hydrogels are thus comprised of a relatively high crosslink density 1st network and an interpenetrating low crosslink density 2nd network (Fig. 1a). The SN and DN hydrogels prepared without nanoparticles were optically clear indicative of a homogeneous morphology associated with curing at low temperatures (T_{prep} < 20 °C) (Fig. 1b).[52,62,63] Upon incorporation of polysiloxane nanoparticles, the DN hydrogels became somewhat opaque and, as expected, more so with the larger ~200 nm nanoparticles. It was observed that DN hydrogels in which the polysiloxane nanoparticles were introduced into the 1st network (*i.e. 50-1* and *200-1*) were relatively more opaque *versus* the corresponding DN hydrogel in which the nanoparticles were incorporated into the 2nd network (*i.e. 50-2* and *200-2*, respectively). Because of the relatively high crosslink density of the 1st network, subsequent integration of polysiloxane nanoparticles was apparently somewhat inhibited. However, *50-2* and *200-2* were more opaque *versus* DN (no nanoparticles), indicating incorporation of some polysiloxane nanoparticles.

VPTT

When heated above its *VPTT*, PNIPAAm hydrogels exhibit an endothermic peak due to breaking of the hydrogen bonds of surrounding water molecules.[64,65] Measured by DSC, the onset (T_o) or the maximum temperature (T_{max}) of the endothermic peak designates the *VPTT*.[66–68] In this way, the *VPTT* of swollen hydrogels were determined (Table 2, Fig. 2). When the hydrogel matrix was changed from a SN ("*SN*") to DN ("*DN*") design, the *VPTT* was not altered. The *VPTT* was also unchanged when polysiloxane nanoparticles were incorporated into DN hydrogels. This effect was similarly observed when ~50 and 200 nm polysiloxane nanoparticles were incorporated into SN hydrogels.[51,52] The lack of change to the *VPTT* is attributed to the discrete nature of the nanoparticles which apparently do not interfere with dissociation of water molecules around the PNIPAAm propyl moieties during heating.

Morphology

The morphology of hydrogels was studied by SEM. Morphology was dramatically changed according to composition (Fig. 3). For *200-1*, pores were notably larger *versus* other hydrogels. This may be the result of its combination of larger nanoparticles (*i.e.* ~200 nm) and higher nanoparticle content (*versus 200-2*) which facilitated the expansion of the pores due to the hydrophobicity of the polysiloxane nanoparticles.

Equilibrium swelling

Equilibrium swelling ratios of the hydrogels were measured gravimetrically from 10 to 50 °C (Fig. 4). At temperatures below the *VPTT* (~33 °C), the hydrogels exist in a swollen state. Enhanced swelling below the *VPTT* is desirable for PNIPAAm-based hydrogels in applications involving transport and delivery. *DN* did not exhibit enhanced swelling *versus SN*. Thus, the enhanced swelling of previously reported DN hydrogel systems likely stems from the electrostatic nature of the ionizable network.[55–57] However, for *200-1*, the swelling ratio was dramatically enhanced below the *VPTT* and without compromising the extent of deswelling above the *VPTT*. The enhanced swelling of *200-1* may be explained by its particularly large pores (Fig. 3).

Kinetic deswelling–re-swelling properties

A rapid and extensive response to thermal modulation (*i.e.* thermosensitivity) of PNIPAAm-based hydrogels is essential for release and delivery applications. The thermosensitivity of hydrogels were determined by measuring the rate and extent to which they deswelled at 50 °C (> *VPTT*) (Fig. 5) and subsequently reswelled at 22 °C (< *VPTT*) (Fig. 6).

DN exhibited an enhanced rate and extent of deswelling *versus SN* due to the former's crosslink inhomogenity. Furthermore, upon incorporation of polysiloxane nanoparticles, the resulting DN hydrogels exhibited an additional increase deswelling. The hydrophobicity of the nanoparticles may facilitate water expulsion during deswelling. DN hydrogels containing ~200 nm nanoparticles exhibited somewhat enhanced deswelling *versus* the corresponding DN hydrogels containing ~50 nm nanoparticles.

As with equilibrium swelling, the rate and extent of reswelling of *DN* are not enhanced *versus* that of *SN*. In most cases, incorporation of polysiloxane nanoparticles into DN hydrogels did not significantly change reswelling behaviour. However, *200-1* exhibited a pronounced increase in the rate as well as extent of swelling. The enhanced thermosensitivity of *200-1* is attributed to its particularly large pores (Fig. 3).

Mechanical properties

Mechanical properties of PNIPAAm-based hydrogels are critical to maintain structural integrity when subjected to mechanical forces both *in vitro* and *in vivo*. During DMA, hydrogel stiffness was measured in terms of the storage modulus (G') as a function of frequency of the applied strain in compression (Fig. 7). G' of *DN* was nearly twice that of *SN*. Because the swelling ratio of *DN* and *SN* are very similar at RT, the enhanced stiffness of *DN* is attributed to its asymmetrically crosslinked network rather than reduced hydration.[56,69] With the exception of *200-1*, incorporation of polysiloxane nanoparticles did not substantially change the RT swelling ratio of DN hydrogels *versus* that of *DN* and *SN*. However, the G' of these DN hydrogels were lower than that of *DN* but remained higher than that of *SN*. It was also observed that for a given nanoparticle size, their incorporation into the 2nd rather than the 1st network produced DN hydrogels with higher G' values. As noted by their relative opacity, less nanoparticles are incorporated into the DN hydrogel when introduced during formation of the 2nd network. Apparently, nanoparticles somewhat alter the asymmetrically crosslinked network of the PNIPAAm matrix so as to relatively diminish its ability to resist deformation.

As was observed for G', the compressive and tensile moduli of all DN hydrogels were greater than that of *SN* (Table 2). Quasi-static compression and tensile tests permitted assessment of strength. Ultimate compressive strength (*UCS*) has been observed to be dramatically enhanced for previously reported DN hydrogels.[55–57] This is attributed to the ability of the asymmetrically crosslinked networks to dissipate the applied force.[56,69] *UCS* and *UTS* of all DN hydrogels were dramatically enhanced *versus* that of *SN*. *200-2* exhibited particularly high strength. However, given the substantially higher swelling of *200-1*, its high moduli and strength values are particularly notable.

Conclusions

Thermoresponsive nanocomposite double network (DN) PNIPAAm hydrogels were prepared by introducing polysiloxane nanoparticles (~50 nm and ~200 nm) during formation of the 1st, tightly crosslinked network or the 2nd, loosely crosslinked network. Nanoparticles were more readily incorporated during formation of the 1st network. Neither the DN matrix nor nanoparticles altered the convenient *VPTT* of conventional, single network (SN) PNIPAAm hydrogels. However, other key physical properties were enhanced. In the absence of nanoparticles, a DN hydrogel (*i.e. DN*) essentially maintained equilibrium swelling and reswelling kinetics but exhibited an increase in the extent and rate of deswelling as well as an increase in hydrogel stiffness and strength. Incorporation of polysiloxane nanoparticles into DN hydrogels further altered these properties depending on size and whether introduced during formation of the 1st or 2nd network. The DN hydrogels formed with ~200 nm polysiloxane nanoparticles in the 1st network (*i.e. 200-1*) exhibited exceptional properties. For *200-1*, equilibrium swelling was dramatically enhanced as well as deswelling–reswelling kinetics. Despite higher equilibrium swelling at RT, its modulus and strength values surpassed that of the SN hydrogel (*i.e. SN*).

Supplementary Material

Refer to Web version on PubMed Central for supplementary material.

Acknowledgments

Funding from NIH/NIDDK (1R21DK082930-01A1) and NSF/ CBET (0854462) is gratefully acknowledged.

Notes and references

1. Wu XS, Hoffman AS, Yager P. J Polym. Sci., Part A: Polym. Chem. 1992; 30:2121–2129.
2. Liu F, Urban MW. Prog. Polym. Sci. 2010; 35:3–23.
3. Hirokawa Y, Tanaka T. J. Chem. Phys. 1984; 81:9379–9380.
4. Hoffman AS, Afrassiabi A, Dong LC. J. Controlled Release. 1986; 4:213–222.
5. Zhang J, Pelton R, Deng Y. Langmuir. 1995; 11:2301–2302.
6. Chaterji S, Kwon K, Park K. Prog. Polym. Sci. 2007; 32:1083–1122. [PubMed: 18670584]
7. Kumar A, Srivastava A, Galaev IY, Mattiasson B. Prog. Polym. Sci. 2007; 32:1205–1237.
8. Eddington DT, Beebe DJ. Adv. Drug Delivery Rev. 2004; 56:199–210.
9. Harmon ME, Tang M, Frank CW. Polymer. 2003; 44:4547–4556.
10. Li Z, He Q, Ma D, Chen H. Anal. Chim. Acta. 2010; 665:107–112. [PubMed: 20417320]
11. Freitas RFS, Cussler EL. Sep. Sci. Technol. 1987; 22:911–919.
12. Zhiming L, Qiaohong H, Dan M, Hengwu C, A SS. Anal. Chem. 2010; 82:10030–10036. [PubMed: 21105674]
13. Chilkoti A, Dreher MR, Meyer DE, Raucher D. Adv. Drug Delivery Rev. 2002; 54:613–630.
14. Nakayama M. Drug Delivery Sys. 2008; 23:627–636.
15. Qiu Y, Park K. Adv. Drug Delivery Rev. 2001; 53:321–329.
16. Kobayashi J, Okano T. Sci. Technol. Adv. Mater. 2010; 11:1–12.
17. Yamato M, Akiyama Y, Kobayashi J, Yang J, Kikuchi T, Okano A. Prog. Polym. Sci. 2007; 32:1123–1133.
18. Callwaert M, Rouxhet PG, Boulange-Petermann L. J. Adhes. Sci. Technol. 2005; 19:765–781.
19. Cunliffe D, Smart CA, Tsibouklis J, Young S, Alexander C, Vulfson EN. Biotechnol. Lett. 2000; 22:141–145.
20. Ista L, Lopez G. J. Ind. Microbiol. Biotechnol. 1998; 20:121–125.
21. Chen J, Yoshida M, Maekawa Y, Tsubokawa N. Polymer. 2001; 42:9361–9365.
22. Gant R, Abraham A, Hou Y, Grunlan MA, Cote GL. Acta Biomater. 2010; 6:2903–2010. [PubMed: 20123136]
23. Gant R, Hou Y, Grunlan MA, Cote GL. J. Biomed. Mater. Res., Part A. 2009; 90A:695–701.
24. Guenther M, Gerlach G, Kuckling D, Kretschmer K, Corten C, Weber J, Sorber J, Suchaneck K-F, Arndt G. Proc. SPIE- Int. Soc. Opt. Eng. 2006; 6167:61670T.
25. Zhang X-Z, Xu X-D, Cheng S-X, Zhuo R-X. Soft Matter. 2008; 4:385–391.
26. Anseth KS, Bowman CN, Brannon-Peppas L. Biomaterials. 1995; 17:1647–1657. [PubMed: 8866026]
27. Xue W, Champ S, Huglin MB. Polymer. 2001; 42:3665–3669.
28. Zeng K, Wang L, Zheng S. J. Phys. Chem. B. 2009; 113:11831–11840. [PubMed: 19670841]
29. Liu Q, Zhang P, Qing A, Lan Y, Shi J, Lu M. Polymer. 2006; 47:6963–6969.
30. Matsuura T, Sugiyama M, Annaka M, Hara Y, Okano T. Polymer. 2003; 44:4405–4409.
31. Yoshida R, Uchida K, Kaneko Y, Sakai K, Kikuchi A, Sakurai Y, Okano T. Nature. 1995; 374:240–242.
32. Xue W, Champ S, Huglin MB, Jones TGJ. Eur. Polym. J. 2004; 40:703–712.
33. Yan Q, Hoffman AS. Polymer. 1995; 36:887–889.
34. Zhang X-Z, Yang Y-Y, Chung T-S. J. Colloid Interface Sci. 2002; 246:105–111. [PubMed: 16290390]
35. Zhang X-Z, Yang Y-Y, Chung T-S. Langmuir. 2002; 18:2538–2542.
36. Serizawa T, Uemura M, Kaneko T, Akashi M. J. Polym. Sci., Part A: Polym. Chem. 2002; 40:3542–3547.
37. Serizawa T, Wakita K, Akashi M. Macromolecules. 2002; 35:10–12.
38. Serizawa T, Wakita K, Kaneko T, Akashi M. J. Polym. Sci., Part A: Polym. Chem. 2002; 40:4228–4235.

39. Zhang X-Z, Yang Y-Y, Chung T-S, Ma K-X. Langmuir. 2001; 17:6094–6099.
40. Kaneko T, Asoh T-A, Akashi M. Macromol. Chem. Phys. 2005; 206:566–574.
41. Satarkar NS, Biswal D, Zach J. Soft Matter. 2010; 6:2364–2371.
42. Schexnailder P, Schmidt G. Colloid Polym. Sci. 2009; 287:1–11.
43. Frimpon RA, Fraser S, Hilt JZ. J. Biomed. Mater. Res., Part A. 2007; 80A:1–6.
44. Zhao Z, Ding Z, Deng Z, Zhen Z, Peng Y, Long X. Macromol. Rapid Commun. 2005; 26:1784–1787.
45. Haraguchi K. Colloid Polym. Sci. 2011; 289:455–473.
46. Harguchi H-J, Li K, Song L. J. Colloid Interface Sci. 2008; 326:41–50. [PubMed: 18672248]
47. Alzari V, Nuvoli D, Scognamillo S, Piccinini M, Gioffredi E, Malucelli G, Marceddu S, Sechi M, Sanna V, Mariani A. J. Mater. Chem. 2011; 21:8727–8733.
48. Lo C-W, Zhu D, Jiang H. Soft Matter. 2011; 7:5604–5609.
49. Zhang X, Pint CL, Lee MH, Schubert BE, Jamshidi A, Takei K, Ko H, Gillies A, Bardhan R, Urban JJ, Wu M, Fearing R, Javey A. Nano Lett. 2011; 11:3229–3244.
50. Kurihara S, Minagoshi A, Nonaka T. J. Appl. Polym. Sci. 1996; 62:153–156.
51. Hou Y, Fei R, Burkes JC, Lee SD, Munoz-Pinto D, Hahn MS, Grunlan MA. J. Biomaterials Tissue Eng. 2011; 1:93–100.
52. Hou Y, Matthews AR, Smitherman AM, Bulick AS, Hahn M, Hou H, Han A, Grunlan MA. Biomaterials. 2008; 29:3175–3184. [PubMed: 18455788]
53. Myung D, Waters D, Wiseman P-E, Duhamel M, Noolandi J, Ta CN, Frank CW. Polym. Adv. Technol. 2008; 19:647–657. [PubMed: 19763189]
54. Gong JP. Soft Matter. 2010; 6:2583–2590.
55. Gong JP, Kurokawa T, Narita T, Kagata G, Osada Y, Nishimura G, Kinjo M. J. Am. Chem. Soc. 2001; 123:5582–5583. [PubMed: 11389644]
56. Gong JP, Katsuyama Y, Kurokawa T, Osada Y. Adv. Mater. 2003; 15:1155–1158.
57. Myung D, Koh W, Ko J, Hu Y, Carrasco M, Noolandi J, Ta CN, Frank CW. Polymer. 2007; 48:5376–5387.
58. Yasuda K, Gong JP, Katsuyama Y, Nakayama A, Tanabe Y, Kondo E, Ueno M, Osada Y. Biomaterials. 2005; 26:4468–4475. [PubMed: 15701376]
59. Weng L, Gouldston A, Wu Y, Chen W. Biomaterials. 2008; 29:2153–2163. [PubMed: 18272215]
60. Zhang X-Z, Wu D-Q, Chu C-C. Biomaterials. 2004; 25:3793–3805. [PubMed: 15020155]
61. Hahn MS, McHale MK, Wang E, Schmedlen RH, West JL. Ann. Biomed. Eng. 2007; 35:190–200. [PubMed: 17180465]
62. Rathjen C-H, Park CM, Goodrich PR, Walgenbach DD. Polym. Gels Networks. 1995; 3:101–115.
63. Kayaman N, Kazan D, Erarslan A, Okay O, Baysal BM. J. Appl. Polym. Sci. 1998; 67:805–814.
64. Shibayama, S-y; Mizutani, M.; Nomura, S. Macromolecules. 1996; 29:2019–2024.
65. Shibayama M, Morimoto M, Nomura S. Macromolecules. 1994; 27:5060–5066.
66. Feil H, Bae YH, Feijen J, Kim SW. Macromolecules. 1993; 26:2496–2500.
67. Otake K, Inomata H, Konno M, Saito S. Macromolecules. 1990; 23:283–289.
68. Singh D, Knuckling D, Choudhary H-J, Adler V, Koul V. Polym. Adv. Technol. 2006; 17:186–192.
69. Tanaka Y, Gong JP, Osada Y. Prog. Polym. Sci. 2005; 30:1–9.

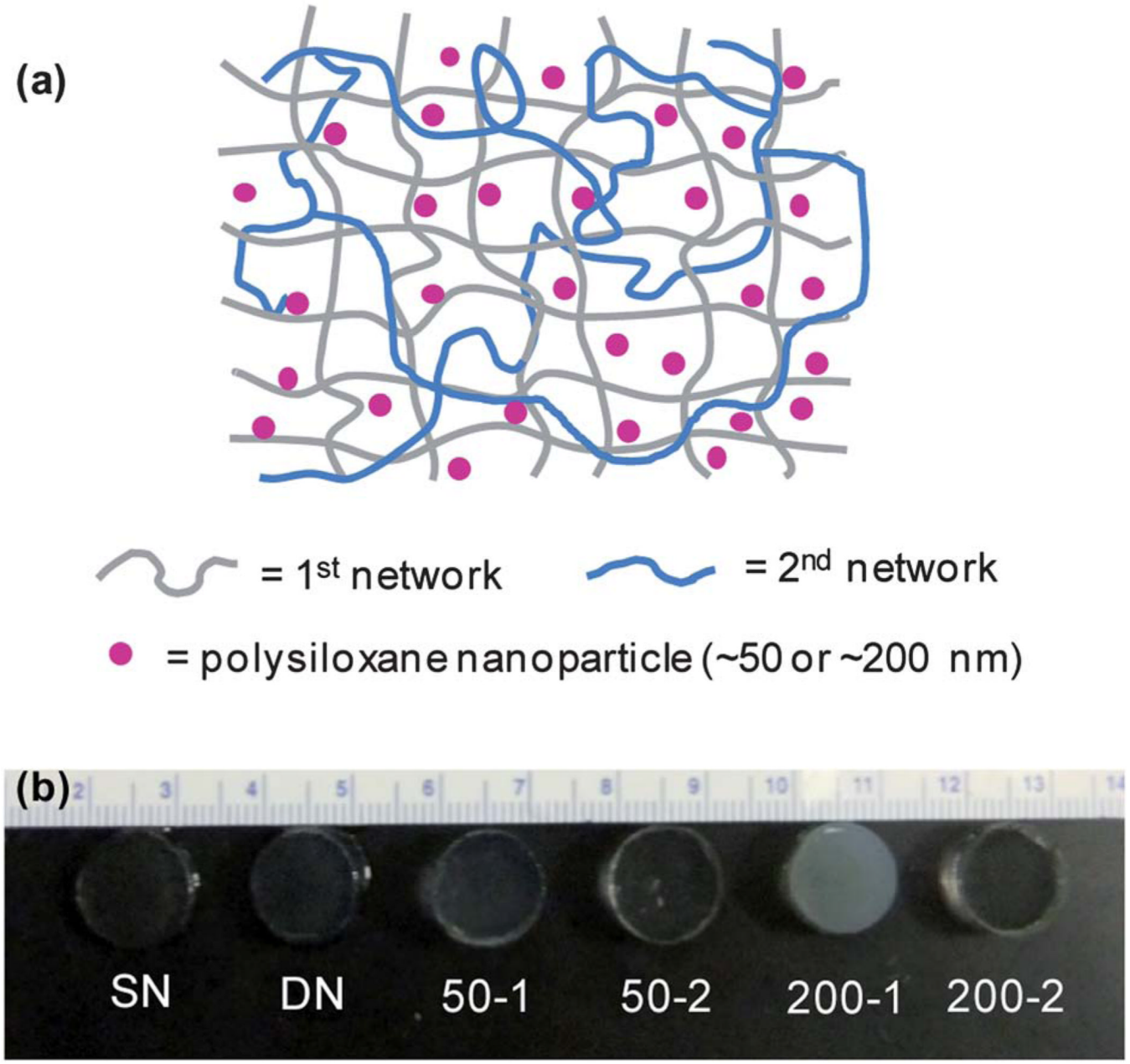

Fig. 1.

(a) Schematic depiction of double network (DN) hydrogels in which polysiloxane nanoparticles were introduced during formation of the "1st network" (*i.e. 50–1 & 200–1*) or the subsequent "2nd network" (*i.e. 50–2 & 200–2*). (b) Photograph of hydrogels series.

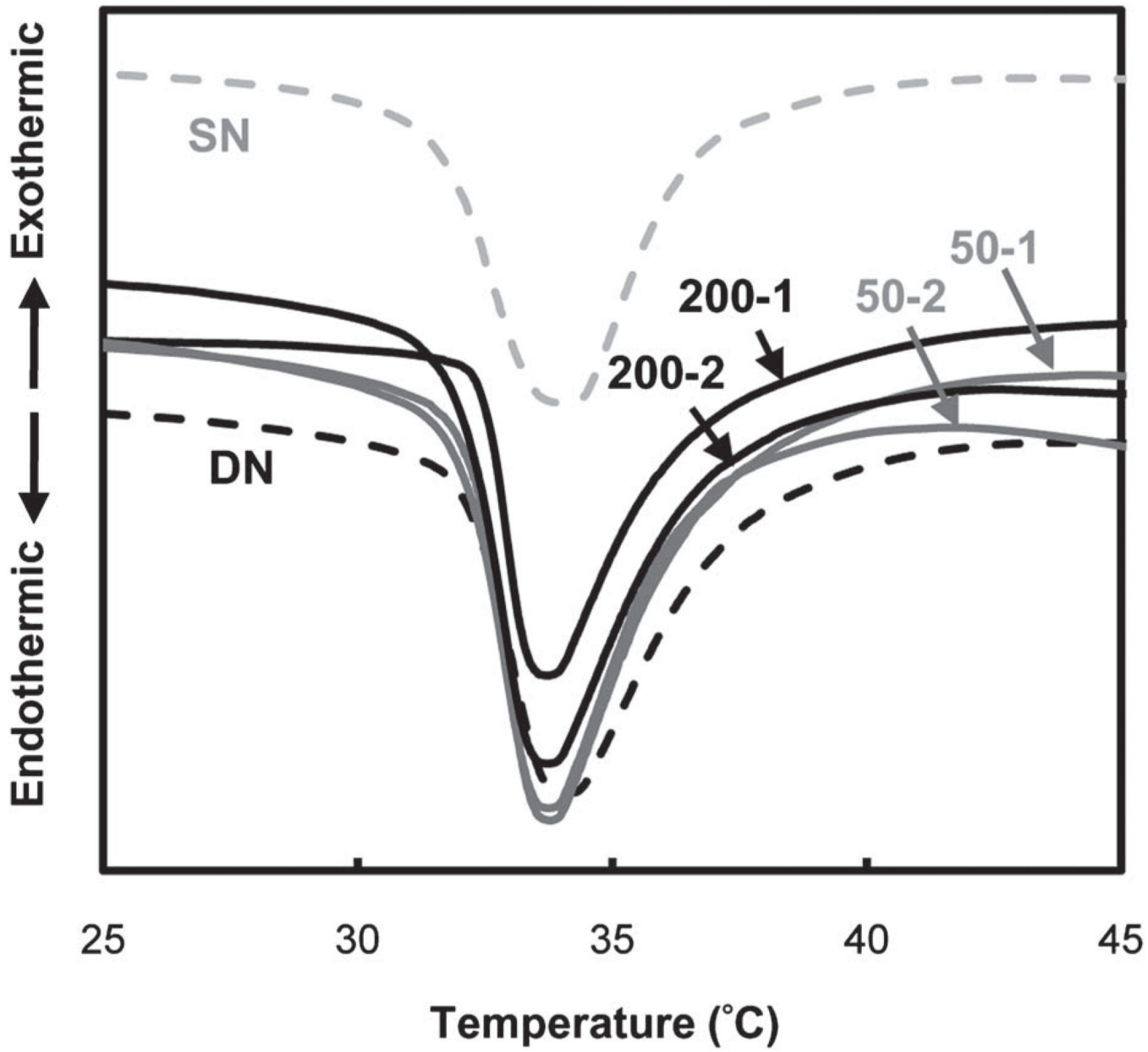

Fig. 2.
DSC thermograms of hydrogels.

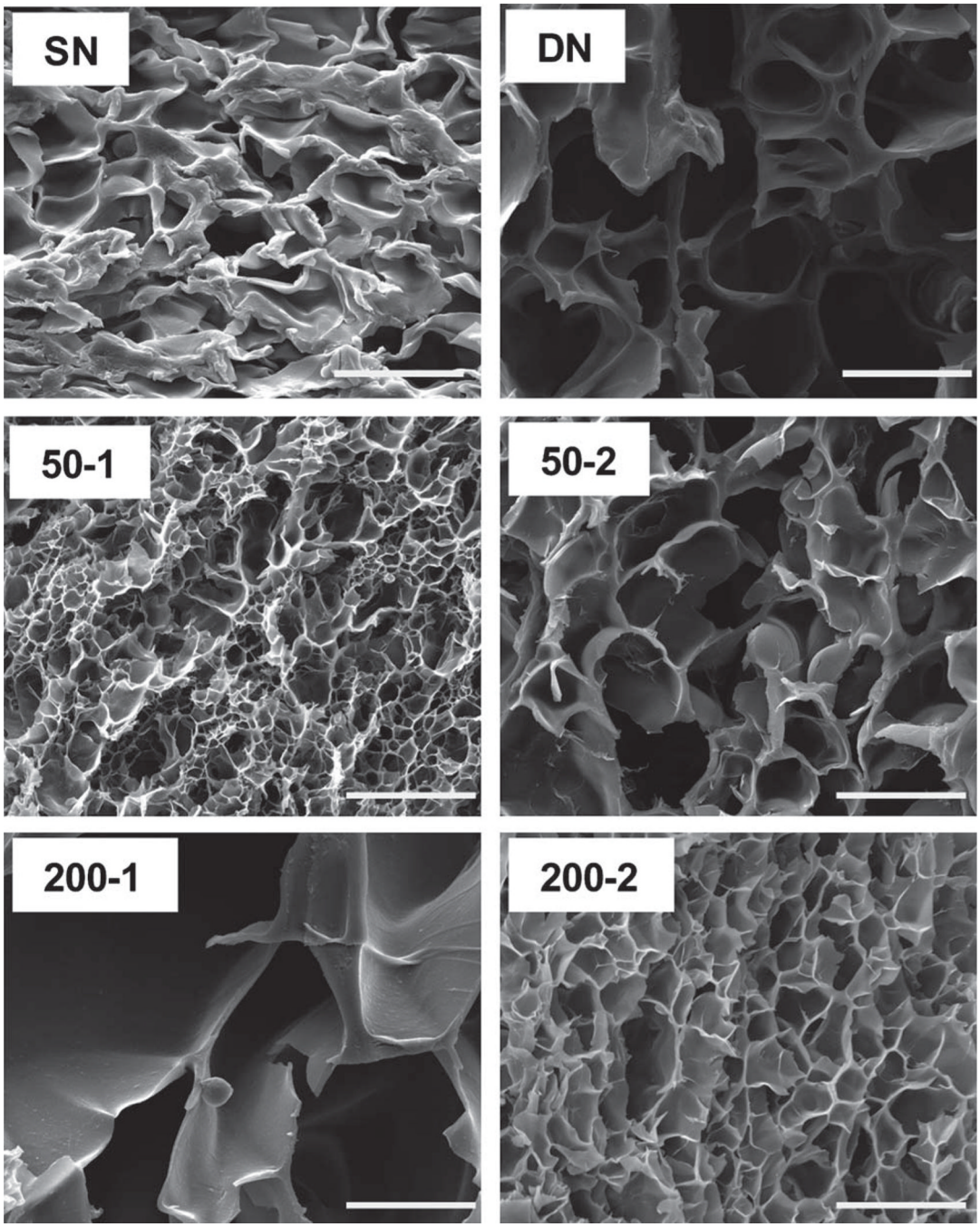

Fig. 3.
SEM micrographs of hydrogels. All scale bars = 20 μm.

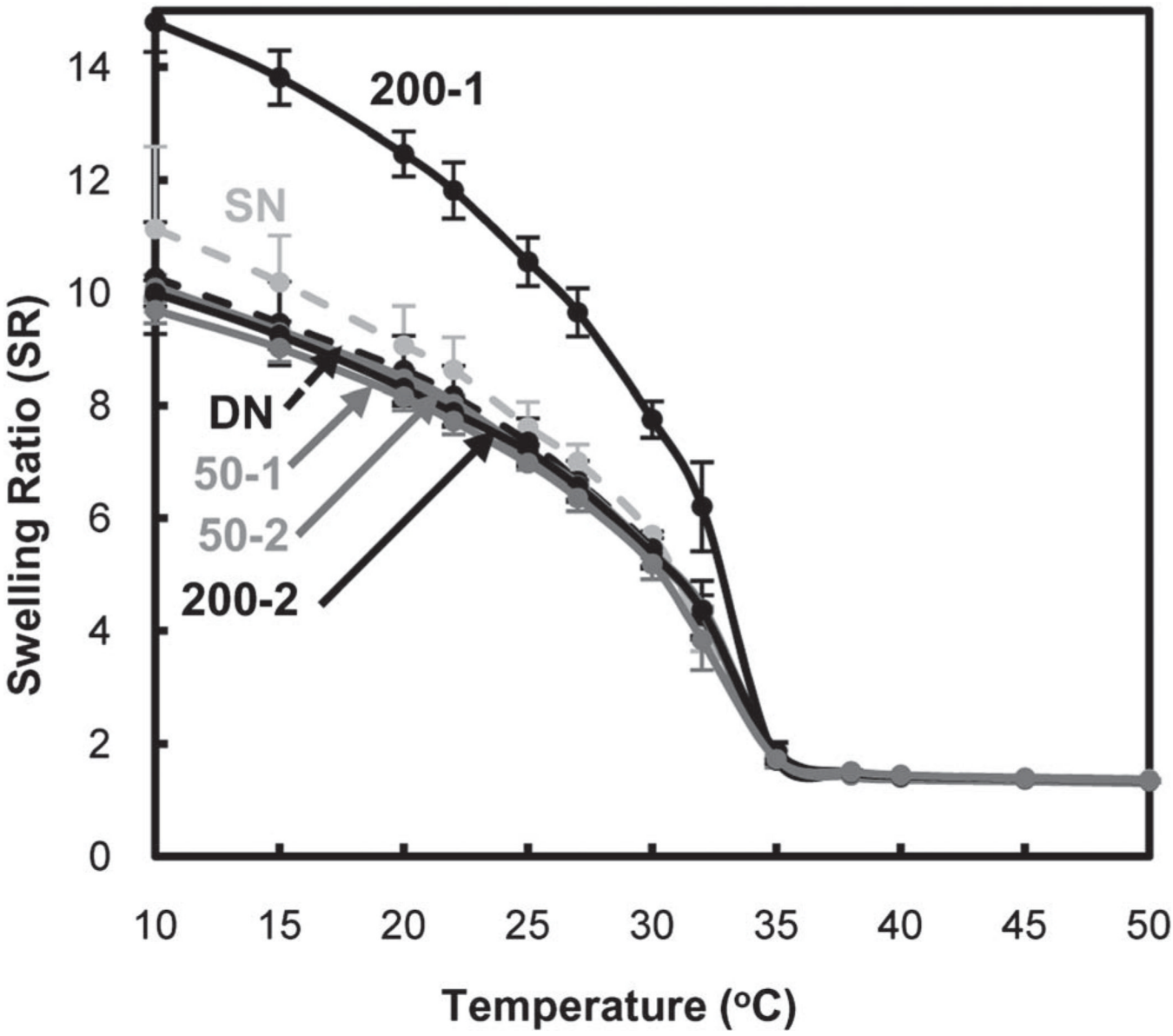

Fig. 4.
Hydrogel equilibrium swelling ratio (by mass).

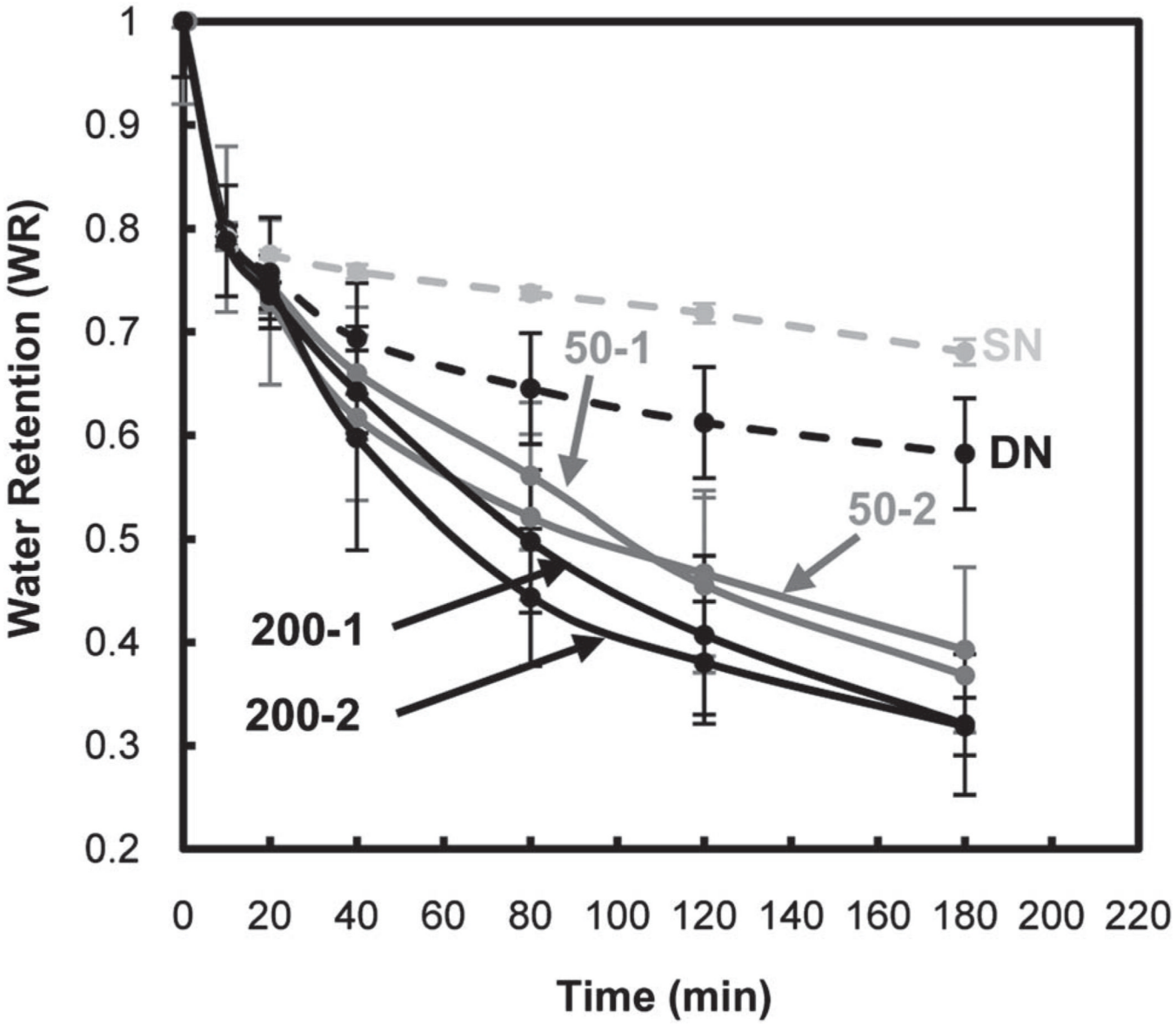

Fig. 5.
Hydrogel deswelling kinetics at 50 °C (by mass).

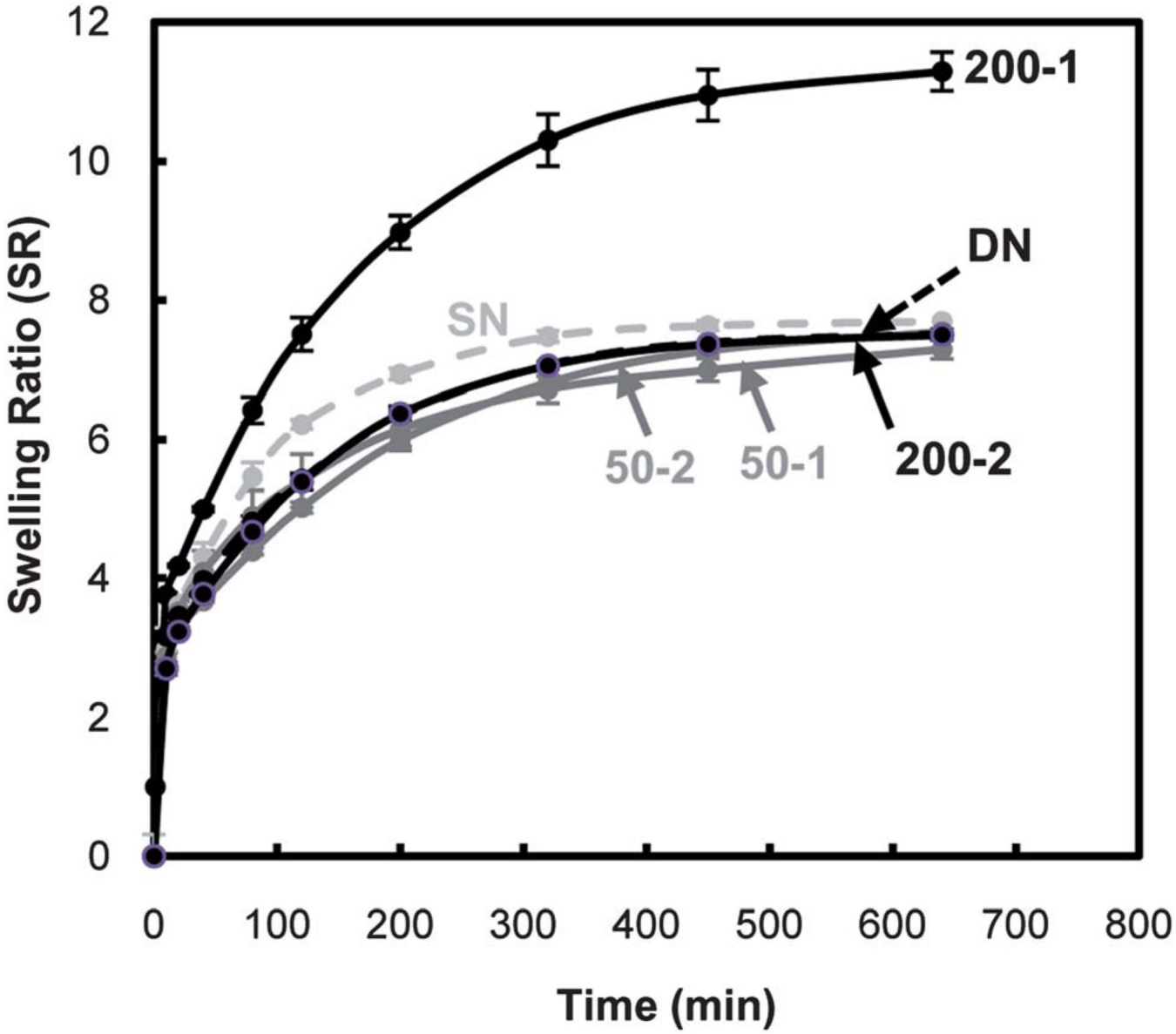

Fig. 6.
Hydrogel reswelling kinetics at 22 °C (by mass).

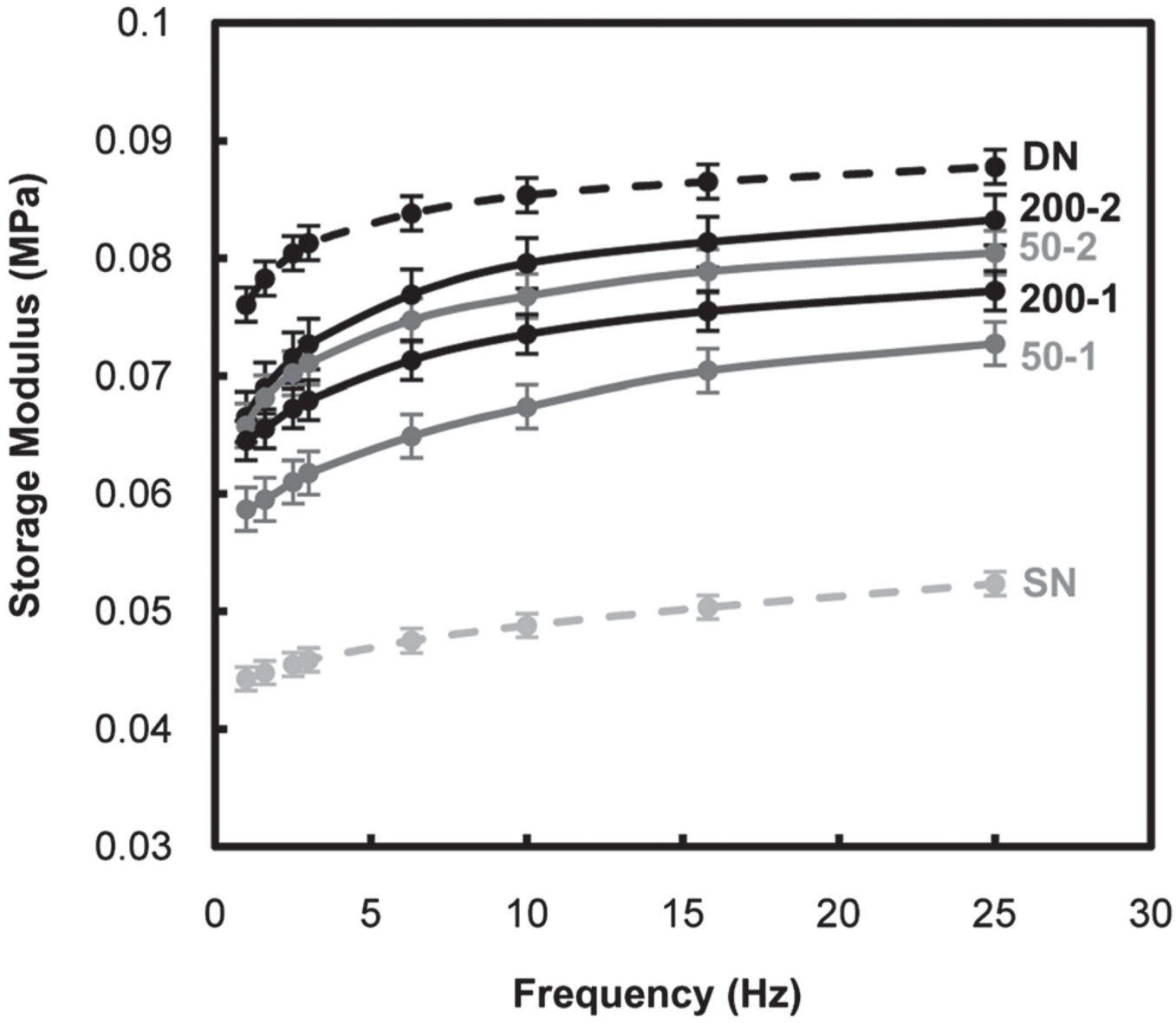

Fig. 7.
Storage modulus (G′) of hydrogels in the compression mode.

Table 1

Hydrogel composition

	1st Network		2nd Network	
Notation	**%BIS**	**NP (size)**	**%BIS**	**NP (size)**
SN	4%	—	—	—
DN	4%	—	0.2%	—
50-1	4%	~50 nm	0.2%	—
50-2	4%	—	0.2%	~50 nm
200-1	4%	~200 nm	0.2%	—
200-2	4%	—	0.2%	~200 nm

Table 2

VPTT and mechanical properties of hydrogels

	VPTT		Compressive Properties			Tensile Properties		
Hydrogel	**T_o (°C)**	**T_{max} (°C)**	**Modulus (kPa)**	**UCS (kPa)**	**%strain @ break**	**Modulus (kPa)**	**UTS (kPa)**	**%strain @ break**
SN	32.0	33.9	81 ± 14	144 ± 12	57 ± 1	19.7 ± 2.0	6.4 ± 0.5	26 ± 3
DN	32.4	34.0	188 ± 7	452 ± 56	52 ± 3	26.6 ± 0.5	8.6 ± 1.4	32 ± 4
50-1	32.5	33.6	162 ± 11	473 ± 59	57 ± 2	21.7 ± 1.6	7.6 ± 1.6	36 ± 3
50-2	32.1	33.5	175 ± 16	474 ± 60	52 ± 1	25.9 ± 1.0	7.9 ± 0.5	31 ± 4
200-1	32.3	33.6	181 ± 7	443 ± 48	51 ± 3	21.0 ± 1.5	7.5 ± 2.7	35 ± 9
200-2	32.2	33.6	165 ± 7	600 ±7	54 ± 2	22.7 ± 1.1	9.9 ± 1.3	40 ± 1